Molecular-dynamics method for the simulation of bulk-solid interfaces at high temperatures

J. F. Lutsko, D. Wolf, S. Yip,* S. R. Phillpot, and T. Nguyen*
Materials Science Division, Argonne National Laboratory, Argonne, Illinois 60439
(Received 29 June 1988)

A new method for the molecular-dynamics simulation of bulk planar interfaces at high temperatures is presented. The method uses the basic Parrinello-Rahman (constant-stress) scheme, modified for the application to inhomogeneous systems. Since our computational cell contains only one interface with two-dimensional (2D) periodic border conditions, we are able to study isolated interfaces all the way up to melting. The interaction between boundaries which may lead to their annihilation at higher temperatures, which is a problem when 3D periodic borders are applied, is thus avoided. As an application, the method is used to study the stability of a grain boundary at high temperatures. Observations on a possible connection between grain-boundary migration and "premelting" are discussed.

I. INTRODUCTION

There are many problems dealing with mechanical and thermal properties of materials where processes which occur at an interface play a critical role. Since the relevent spatial region for such phenomena, although sometimes difficult to define precisely, is frequently only a few atomic layers in extent, molecular-level considerations of structure and dynamics take on central importance in studies of interfacial systems. The atomistic methods of molecular dynamics (MD) and Monte Carlo, in principle, can provide those details if sufficiently realistic interatomic potentials are available.[1,2] However, it is a fundamental difficulty in the simulation approach to treat properly the interactions between the interfacial region and the surrounding bulk matter.

In practice the problem arises in the formulation of the border conditions for the simulation cell. One is faced with the simultaneous requirements of a small simulation cell for economy of computations and a large cell so the interfacial region is not perturbed artificially by the action of the cell borders. In simulation studies of grain boundaries, bicrystal model are used in which a planar interface, infinite in extent, is represented by a finite simulation cell with border conditions which are periodic in the two directions along the interface (the x and y borders).[3] In the direction perpendicular to the interface, the z borders are expected to simulate the bulk media on either side of the interface. If one imposes periodic conditions on these borders as well [thus imposing three-dimension (3D) periodic border conditions on the system], then there will be necessarily two interfaces in the cell, a situation considered unsatisfactory since the two interfaces can influence each other and, in the case of grain boundaries, at high temperatures even annihilate each other. Also, because of the coupling through the z border, the two halves of the bicrystal are not free to translate relative to one another arbitrarily. Besides the problem of avoiding two interfaces, one also needs the z borders to be sufficiently flexible to accommodate any deformation or volume change that may occur in the (inhomogeneous) interfacial region during the simulation. At present none of the borders in use can be said to have these properties.

In this paper we present a new method of molecular-dynamics simulation, applicable to the study of structural properties of solid interfaces at finite temperature and stresses, which avoids some of these problems. The basis of the method is a treatment of the z borders that allows the simulation cell to expand or contract in the z direction according to the stresses produced in the cell, as well as independent translations of the two halves of the bicrystal. The approach we use is a variation of the Lagrangian formulation proposed by Parrinello and Rahman in which the vectors defining a homogeneous simulation cell can respond to any imbalance between the internal stress and a prescribed external stress.[4] In our case we treat the cell as periodic in the x and y directions with fixed planar area, while the cell length in the z direction is a dynamical variable and the z borders are not periodic, thus imposing 2D periodic border conditions (2D PBC's). Atoms are placed beyond the z borders of the simulation cell as a continuation of the bulk regions and they are allowed to move as a rigid unit. Thus the simulation cell contains a single isolated interface, and it will accommodate dimensional changes normal to the interface and translational motions parallel to the interface plane.

A central question in the simulation of grain-boundary structures has been the nature of a structural transition which has been claimed to exist in the range of $0.5T_m$ and above, where T_m is the bulk ideal-crystal melting point.[5-9] Simulations using 3D PBC's (Refs. 5 and 6) and 2D (Ref. 7) PBC's with fixed z borders have been carried out, leading to results which all show a significant thermal disordering; however, one cannot conclude whether the interface undergoes a melting transition of its own.[10] Part of the difficulty clearly stems from the treatment of the z borders. In the case of 3D periodic borders, enhanced interaction, thermally activated, between the two boundaries in the cell gives rise to boundary migration.[5,8,11] In the case of fixed borders, relief of thermal stress induced at the interface is a concern.[12]

The plan of this paper is as follows. In Sec. II we de-

scribe the model system for interface simulations in some detail. In Sec. III the results of the equilibration of an ideal crystal at elevated temperatures using the 2D PBC model are compared to results from an identical simulation performed with 3D PBC's. In Sec. IV the equilibration of a grain boundary is investigated while the kinetics of the grain boundary near the melting point is discussed in Sec. V. Finally, in Sec. VI, we present some conclusions on the connection between the observed grain-boundary migration and earlier studies on premelting phenomena in grain boundaries.

II. SIMULATION MODEL

An important problem in simulating an isolated interface is its proper embedding in a bulk environment. As pointed out in the Introduction, this requires the modification of the commonly used 3D PBC's to account for the inhomogeneity in the z direction of the simulation cell introduced by the presence of the interface (which lies in the x-y plane; see Fig. 1). The inhomogeneity may be structural (such as a volume change in the interface region) or chemical (for example, for dissimilar-material interfaces). As long as the interface is planar and coherent, i.e., as long as it can be characterized by a periodic planar unit cell, 2D periodic borders are appropriate in the x-y plane. In contrast to 3D PBC's they reflect the physical nature of planar defects.

The geometrical layout of our simulation cell (Fig. 1) combines 2D PBC's in the plane of the interface with its embedding in bulk-crystal regions. For that purpose the simulation cell is subdivided into two regions, a region I in which the equations of motion are solved explicitly for all atoms and a region II consisting of two rigid blocks,

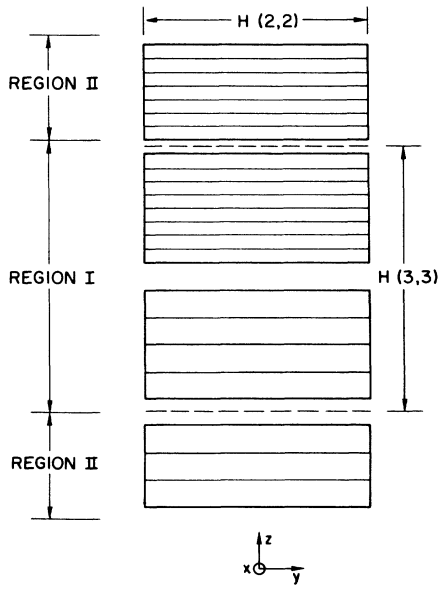

FIG. 1. Schematic diagram of the region-I–region-II simulation method. An interface between different materials is indicated. Also shown are the simulation-cell dimensions in the y and z directions [$H(2,2)$ and $H(3,3)$].

one on either side of the interface. The extent of the blocks in the z direction is obviously determined by the range (i.e., cutoff radius) of the potential. Such a region-I–region-II strategy is commonly used in the zero-temperature (lattice statics) simulation of grain boundaries.[12,13] The challenge at hand lies in the finite-temperature simulation of the proper *dynamical* behavior of this complex geometrical setup.

Whereas the atoms in region I are individually allowed to move in response to the forces acting on them, the atoms in region II are held fixed at their ideal-crystal positions. However, each rigid block is permitted to move as a unit in response to the total force exerted by region I. Initially, the positions of the rigid blocks are fixed by taking the distance between the outermost plane of region I and the first plane of region II to be the perfect-crystal interplanar spacing appropriate for the simulation temperature.

The movement of the rigid blocks in the z direction is conceptually rather different from their translations parallel to the interface plane. Whereas the movement in z is governed by the *pressure* exerted on the rigid blocks by region I, the sliding of each block is controlled by the *force* exerted on the block across the region-I–region-II border. Thus, the z movement is treated in the usual manner of the Parrinello-Rahman method,[4] while each block translates in the x-y plane as a single particle with an effective mass. In this formulation, each block contributes 2 degrees of freedom to the system.

While a general Parrinello-Rahman treatment is possible (in which all six walls of the simulation cell move as corresponding pairs) it is not generally desirable in the simulation of isolated interfaces surround by bulk regions since the x-y dimensions of the interfacial region are fixed by the lattice parameter(s) of these bulk regions. These lattice parameters are input parameters for our simulation. They are determined independently from a constant-pressure simulation of a bulk ideal crystal (with 3D PBC's) at the desired temperature for the same interatomic force model. Having thus fixed the planar (x-y) dimensions of the simulation cell, the system is allowed to expand or contract in the z direction.

The following mathematical formulation of the dynamical equations for our model system follows rather closely the Parrinnello-Rahman scheme with modifications indicated as necessary. First, in order to characterize the translational configurations of the rigid blocks, we define the vectors $\mathbf{T}^+=(T_x^+, T_y^+, T_z^+)$ and $\mathbf{T}^-=(T_x^-, T_y^-, T_z^-)$ for the upper (+) and lower (−) block, respectively. Then, at fixed volume and, for simplicity, for pairwise interactions between the atoms, the potential energy of the system may be written as follows:

$$V_T(\{\mathbf{q}_i\})=\tfrac{1}{2}\sum_{\substack{i,j\in \mathrm{I}\\ i\neq j}} V(\mathbf{q}_{ij})+\tfrac{1}{2}\sum_{\substack{i\in \mathrm{I}\\ j\in \mathrm{II}}} V(\mathbf{q}_{ij}) \tag{2.1}$$

with

$$\mathbf{q}_{ij}=\mathbf{q}_i-\mathbf{q}_j,\quad i,j\in \mathrm{I} \tag{2.2}$$

or

$$\mathbf{q}_{ij}=\mathbf{q}_i-(\mathbf{q}_{j0}+\mathbf{T}^{\pm}),\quad i\in \mathrm{I}, j\in \mathrm{II}\ , \tag{2.3}$$

where the subscript "0" indicates that the atoms in region II are at ideal-crystal lattice positions. Thus, while the atom positions in the rigid blocks are fixed relative to their respective centers of mass, the two centers of mass, characterized by $\mathbf{T}^{\pm}$, are dynamical variables. These allow the independent translation of the two halves of the bicrystal. As illustrated in Sec. V below, the six variables in $\mathbf{T}^{\pm}$ represent very important degrees of freedom of the interface system.

The key to the Parrinello-Rahman method[4] is to introduce a 3×3 matrix, $\underline{H}$, the columns of which are vectors describing the direction and length of the walls of the simulation cell (Fig. 1). The elements of $\underline{H}$, are then treated as dynamical variables. New reduced particle coordinates, $\{\mathbf{s}_i\}$, are then defined via

$$\mathbf{q}_i=\underline{H}\cdot\mathbf{s}_i \ , \tag{2.4}$$

where, because of the periodicity in x and y,

$$\begin{aligned} -0.5<s_{ix}\le 0.5 \ , \\ -0.5<s_{iy}\le 0.5 \ . \end{aligned} \tag{2.5}$$

The vectors $\mathbf{T}^{+}$ are also scaled, thus defining the reduced translation vectors $\mathbf{t}^{\pm}$

$$\mathbf{T}^{\pm}=\underline{H}\cdot\mathbf{t}^{\pm} \ . \tag{2.6}$$

Finally, Eq. (2.3), which describes the separation between particles in region I and region II, becomes

$$\mathbf{s}_{ij}^{T}=\mathbf{s}_i-(\mathbf{s}_j^0+\mathbf{t}^{\pm}) \ , \tag{2.7}$$

where it is understood that $\mathbf{s}_j^0$ is now held fixed. Equations (2.1)–(2.7) specify the potential energy for the system

$$V_T(\{\mathbf{s}_i\},\mathbf{t}^{\pm},\underline{H})=\tfrac{1}{2}\sum_{\substack{i\in\mathrm{I}\\ i\neq j}}\sum_{j\in\mathrm{I}} V(\underline{H}\cdot\mathbf{s}_{ij}) +\tfrac{1}{2}\sum_{i\in\mathrm{I}}\sum_{i\in\mathrm{II}} V(\underline{H}\cdot\mathbf{s}_{ij}^{T}) \ . \tag{2.8}$$

The equations of motion for the system may be derived from the Lagrangian formalism by introducing the Lagrangian,

$$L=K-V_T \ , \tag{2.9}$$

where the kinetic energy, K, is given by

$$K=\frac{m}{2}\sum_{i\in\mathrm{I}}\left[\frac{d}{dt}\underline{H}\cdot\mathbf{s}_i\right]^2+\tfrac{1}{2}M_W\mathrm{Tr}(\dot{\underline{H}}\cdot\dot{\underline{H}}^{T}) +\tfrac{1}{2}M_T\sum_{\pm}\left[\frac{d}{dt}\underline{H}\cdot\mathbf{t}^{\pm}\right]^2 . \tag{2.10}$$

Here, we have introduced an adjustable "wall mass," M_W, associated with the $\underline{H}$ matrix and a T vector mass M_T. In the simulation these masses are adjusted, by trial and error, so that the variables associated with them fluctuate on the same time scales as the particles. (Typically, M_W and M_T are about 10 particle masses.)

From the usual Lagrangian formalism, one finds the following equations of motion of the particles in region I:

$$m\ddot{\mathbf{s}}_i=-\sum_{j\in\mathrm{I,II}} X_{ij}\mathbf{s}_{ij}-m\underline{G}^{-1}\cdot\dot{\underline{G}}\cdot\dot{\mathbf{s}}_i \quad (i\in 1) \ , \tag{2.11}$$

where

$$X_{ij}=[dV(q_{ij})/dq_{ij}](1/q_{ij}) \ , \tag{2.12}$$

and

$$\underline{G}=\underline{H}^{T}\cdot\underline{H} \ . \tag{2.13}$$

The positions in region II are given by

$$\mathbf{s}_i=\mathbf{s}_i^0+\mathbf{t}^{\pm} \ . \tag{2.14}$$

The equations of motion for the scaled T vector are

$$M_T\ddot{\mathbf{t}}^{\pm}=\sum_{i\in\mathrm{I}}\sum_{j\in\mathrm{II}^{\pm}} X_{ij}\mathbf{s}_{ij}-M_T\underline{G}^{-1}\cdot\dot{\underline{G}}\dot{t}^{\pm} \ . \tag{2.15}$$

$\mathbf{t}^{\pm}$ is seen to move in response to the total force acting between region I and region II. Finally, the equations of motion for the walls are obtained:

$$M_W\ddot{\underline{H}}=\left[\sum_{i\in\mathrm{I}} m\mathbf{v}_i\mathbf{v}_i+\sum_{\pm}M_T(\dot{\underline{H}}\cdot t^{\pm})(\dot{\underline{H}}\cdot\mathbf{t}^{\pm})-\tfrac{1}{2}\sum_{\substack{i,j\in\mathrm{I}\\ i\neq j}}(X_{ij}/q_{ij})\mathbf{q}_{ij}\mathbf{q}_{ij}-\tfrac{1}{2}\sum_{i\in\mathrm{I}}\sum_{j\in\mathrm{II}}(X_{ij}/q_{ij})\mathbf{q}_{ij}\mathbf{q}_{ij}\right]\cdot(\underline{H}^{T})^{-1} \ . \tag{2.16}$$

The terms in the small parentheses are recognized as the pressure tensor generalized to include the T vectors. The H matrix, or walls of the simulation cell, thus move in response to the stress acting on region I as in the Parrinello-Rahman scheme.

The Hamiltonian for this system may be derived from its Lagrangian and energy is, of course, conserved by these equations. The systems thus behaves physically just as well as a homogeneous 3D periodic system, even to the point of conserving energy. However, the Parrinello-Rahman constant-pressure scheme introduces an unphysical aspect in the simulation of interfacial systems; it requires that volume and strain fluctuations take place *homogeneously*. However, as described in the Introduction, the most important difference between interfacial and bulk systems is the inhomogeneity of the interfacial system perpendicular to the interface.

This problem can best be seen by considering the separation, in real space, between two particles in region II^{+}. For two particles i and j Eqs. (2.4) and (2.14) yield

$$\begin{aligned} \mathbf{q}_i-\mathbf{q}_j&=\underline{H}\cdot(\mathbf{s}_i^0+\mathbf{t}^{+})-\underline{H}\cdot(\mathbf{s}_j^0+\mathbf{t}^{+}) \\ &=\underline{H}\cdot(\mathbf{s}_i^0-\mathbf{s}_j^0) \ . \end{aligned} \tag{2.17}$$

Thus, although in s space the distance between the particles is fixed, in real space their separation is not fixed but

depends on $\underline{H}$. Since, generally, $H(1,1)$ and $H(2,2)$ are held constant to fix the planar area, Eq. (2.17) is only a problem for the z components

$$q_{iz}-q_{jz}=\underline{H}(3,3)(s^0_{iz}-s^0_{jz}) . \tag{2.18}$$

However, $H(3,3)$ is obviously affected by the inhomogeneity in the z direction. Therefore, the rigid blocks do not behave as if they were bulk ideal-crystal regions. This unphysical behavior of the rigid blocks due to the inhomogeneity in the z direction thus necessitates the following *ad hoc* modification of Eqs. (2.14) and (2.15)

$$\begin{aligned} q_{iz}&=q_{iz}+T_z^{\pm} , \\ T_z^{\pm}&=\pm[H(3,3)-H_0(3,3)]/2 , \end{aligned} \tag{2.19}$$

where $H_0(3,3)$ is defined as the initial value of $H(3,3)$.

These equations are written in real space, as opposed to s space, since it is the scaling by $\underline{H}$ which caused the original problem. Although now the system no longer conserves energy (since the equations of motion cannot be derived from a Hamiltonian), these equations give the desired behavior as we shall demonstrate below. Physically, they require that the rigid blocks are at a fixed position with respect to $H(3,3)$. Since, as pointed out above, the correct lattice parameters for the bulk regions are input parameters, any change in $H(3,3)$ is due to the interface. Equation (2.19) takes account of this by holding fixed the interplaner spacings in region II.

It should be noted that now T_z is no longer a dynamical variable. To be consistent, its kinetic energy term is dropped from the Lagrangian, Eq. (2.10), and from the stress appearing in Eq. (2.16). It is henceforth fixed by the constraint in Eq. (2.19).

Finally, we point out certain caveats applied in the implementation of this scheme. A damping term is added to the equations of motion of the walls and the T vectors as these variables otherwise cause the system to "remember" fluctuations in the volume and translation leading to unphysical effects. In addition, a thermostat is applied to the system to maintain constant temperature, as is common in 3D PBC simulations. However, one does not want to thermostat the rigid blocks in region II thus inducing artificial relative translations of the halves of the bicrystal; they therefore drain energy from the system causing the planes next to the border to be somewhat cooler than the rest of the system. To circumvent this problem, we subdivide region I approximately into thirds in the z direction and thermostat each third separately. The central third contains the interface and is the one of greatest physical importance. The simulation cell is chosen large enough that the effects of the interface are confined to this innermost region with the rest of region I and all of region II serving only to provide the necessary environment for the interface. It appears that once the system reaches equilibrium, a single thermostat may be sufficient. This has not been tested, however, and more work is necessary to ascertain whether this is actually the case.

III. IDEAL-CRYSTAL EQUILIBRATION

Although at zero temperature the model we have described produces the correct energy, forces and volume, it is not clear, *a priori,* how realistically the system will behave at finite temperatures. To investigate this, we have performed molecular-dynamics simulations of an ideal crystal using both 3D PBC's and 2D PBC's. The 3D PBC simulation was performed using the Parrinello-Rahman constant-pressure scheme and the resulting lattice parameter was then used as input in the 2D PBC simulation. As was described above, the planar area in the 2D PBC simulation was fixed and the length of the simulation cell was allowed to fluctuate in the z direction. All of our simulations were performed with a Lennard-Jones potential parametrized to represent Cu ($\varepsilon=0.167$ eV and $\sigma=2.3151$ Å). The zero-temperature lattice parameter, a_0, for this potential is 3.616 Å. The potential was cut off at $1.49a_0$ and shifted to cause the force to go smoothly to zero at the cutoff. The region I of the simulation cell consists of 32 (001) planes parallel to the x-y plane. Each plane contains 29 atoms making a total of 928 atoms. At zero temperature, the cell is square and the x, y, and z dimensions are $3.808a_0$, $3.808a_0$, and $16.000a_0$, respectively. Because the interplanar spacing (in the z direction) is $0.5a_0$, regions $\text{II}^{\pm}$ contain three planes each thus satisfying the criterion that the z dimension of region II is greater than the cutoff. This geometry was chosen as it is the reference system for the grain-boundary simulations to be described below, where the importance of the large planar unit cell and well-defined lattice planes will be discussed.

Because the primary application of our MD model is to spatially inhomogeneous systems, it is necessary to monitor properties, such as the potential energy and temperature, locally. We therefore divide the simulation cell into 32 slices in the z direction with each slice containing one lattice plane. Properties were then tabulated independently for each slice as well as for the whole system. This yields a profile of the distribution of the various properties in the z direction.

The comparisons of the 3D PBC and 2D PBC ideal-crystal simulations presented below are made for identical runs at 900 K ($\sim 75\%$ of melting) for 5000 time steps. (This melting point is the temperature at which the system spontaneously melts when the temperature is raised at the same rate as was used in all simulations described here.) The time step size of 0.0365 psec provides energy conservation to six significant figures in the 3D PBC system. Instantaneous properties were tabulated throughout the runs while time-averaged properties were calculated for the last 4000 steps, after initial transients had died away (i.e., after the system had equilibrated). Figure 2 shows the time-averaged potential-energy distributions in both the 3D and 2D systems. One sees that over most of the simulation cell, the distribution of potential energy shows similar fluctuations about the same mean value in both systems, the only exception being near region II in the 2D system. The atoms which interact directly with region II tend to have the same potential energy as the static atoms in region II which understandably is lower

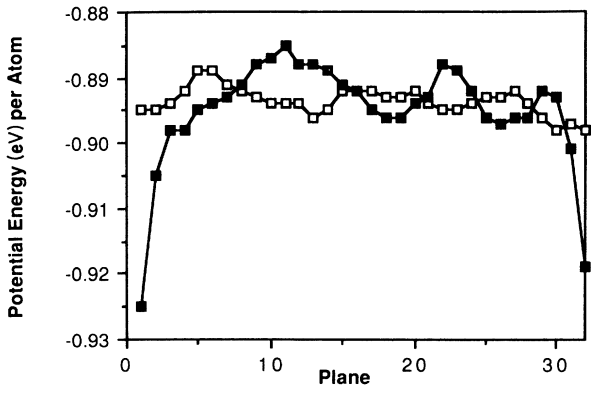

FIG. 2. Average-potential-energy profile for the 3D PBC ideal crystal (open symbols) and the 2D PBC ideal crystal (solid symbols) after 5000 time steps.

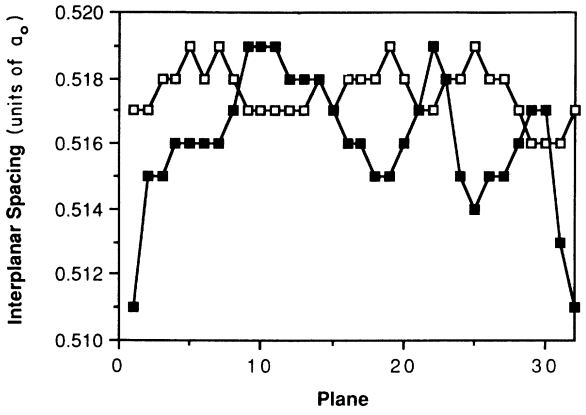

FIG. 4. Average interplanar spacings for the 3D PBC ideal crystal (open symbols) and the 2D PBC ideal crystal (solid symbols) after 5000 time steps.

than the mean value in region I. (At the lattice parameter of 3.744 Å, which is appropriate for 900 K, the energy of an atom in region II is -0.996 eV.) In practice, the spatial extent of this effect is such that region I has to be large enough to ensure that the interface is at least two cutoff radii from region II. In making quantitative comparisons between the 2D and 3D ideal crystals, we will therefore neglect the contribution of the outermost three planes in region I to the overall system properties.

Neglecting the outermost three planes in region I, we find that the average potential energy in the 2D ideal crystal is -0.8923 eV while in the 3D system it is -0.8937 eV. Considering that (a) the 2D system uses three thermostats whereas there is only one in the 3D system and (b) the fact that the input lattice parameter in the 2D simulation is only known to finite precision, this agreement is excellent. Figures 3 and 4 show the time-averaged profiles of the temperature and interplanar spacings, respectively. We see again that the profiles are essentially the same in the two systems with the exception that the interplanar spacing, again, shows a region II effect at the outermost planes. Because the atoms in region II do not individually vibrate there is less thermal expansion at the region-I–region-II interface than in the bulk. However, this effect is again limited to the region I planes immediately adjacent to region II. Neglecting the outermost three planes in region I, the overall average interplanar spacing is $0.5164a_0$ compared to $0.5168a_0$ in the 3D system. The variance (in time) is found to be $0.0004a_0$; i.e., the interplanar spacings are indistinguishable in the two systems.

Finally, we consider the static structure factor, $S(\mathbf{k})$, which is the Fourier transform of the density. The square of its magnitude is given by

$$|S(\mathbf{k})|^2 = \left[\frac{1}{N}\sum_i \cos(\mathbf{k}\cdot\mathbf{q}_i)\right]^2 + \left[\frac{1}{N}\sum_i \sin(\mathbf{k}\cdot\mathbf{q}_i)\right]^2, \tag{3.1}$$

where, for the overall $S(\mathbf{k})$, the sums include all atoms, while for the planar $S(\mathbf{k})$ the sums include only the atoms in a plane. When the wave vector is chosen to be a reciprocal lattice vector, the magnitude of $S(\mathbf{k})$ is a measure of the crystalline order. In our simulations, $\mathbf{k}$ was chosen to be a reciprocal lattice vector in the x-y plane, so the magnitude of $S(\mathbf{k})$ [henceforth denoted simply as $S(\mathbf{k})$], measures the planar order. At zero temperature $S(\mathbf{k})$ is equal to unity, while in the liquid it fluctuates close to zero. Figure 5 shows the instantaneous $S(\mathbf{k})$ plane by plane at the end of the simulations. Again, agreement between the 2D PBC and 3D PBC results indicates that the planar structure in the two systems is identical.

Other properties, such as the pressure, mean-squared displacement in the x-y plane and mean-squared displacement in the z direction, behave in the same qualitative manner as those shown above. Typically, a small effect due to the region-I–region-II interface is observed, and is confined to the two or three planes adjacent to region II. As the temperature is raised, these effects may extend an additional one or two planes into region I, but even at 1200 K (approximately 95% of melting) they are confined to less than two cutoff radii of region II.

Finally, we note that while the fluctuations, from one

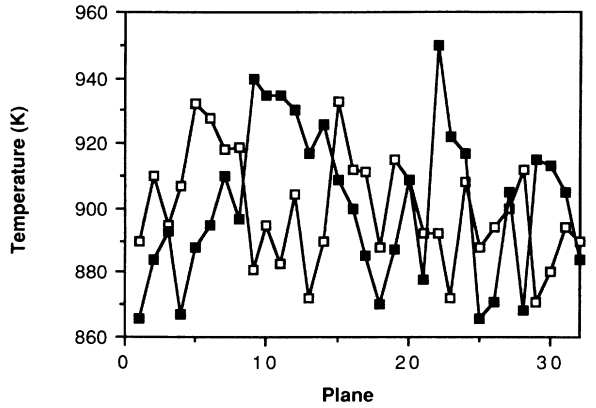

FIG. 3. Average-temperature profile for the 3D PBC ideal crystal (open symbols) and the 2D PBC ideal crystal (solid symbols) after 5000 time steps.

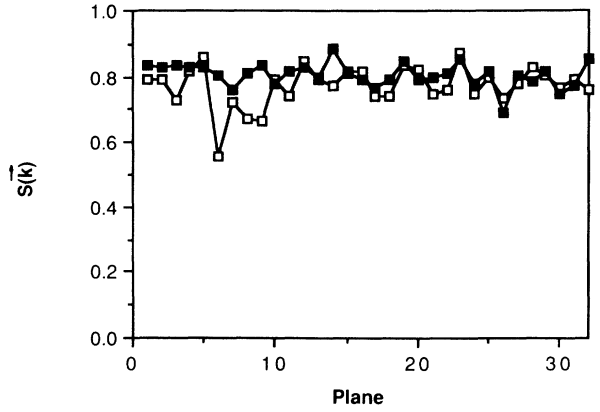

FIG. 5. Instantaneous $S(\mathbf{k})$ profile for the 3D PBC ideal crystal (open symbols) and the 2D PBC ideal crystal (solid symbols) after 5000 time steps.

plane to another, in the various properties are of similar magnitude in the 2D and 3D systems, they do appear to be larger in the 2D system in some properties, such as the energy. These appear to be caused by the dynamical differences in the 2D and 3D systems. Specifically, the 2D system contains degrees of freedom due to the possibility of the independent translation of the top and bottom halves of the crystal afforded by the T vectors which are not present in the 3D system. These additional degrees of freedom give rise to additional fluctuations in quantities which are dependent on correlations between planes, such as the potential energy and interplanar spacing, while leaving unaffected properities such as the temperature and structure factor which are not so strongly dependent on interplanar coupling.

IV. GRAIN-BOUNDARY EQUILIBRATION

Having demonstrated that the 2D PBC model accurately reproduces the properties of an (homogeneous) ideal crystal, we now consider the equilibration of an (inhomogeneous) interfacial system. We have performed molecular-dynamics simulations of the so-called $\Sigma 29$ twist grain boundary on the (001) plane over a range of temperatures, both to investigate the 2D model as applied to an interfacial system and to investigate the high-temperature stability of the grain boundary. (In the usual terminology, Σ is the inverse density of coincidence lattice sites.) The two factors motivating the choice of this grain boundary are its relatively large planar unit cell and the large interplanar spacing of the (001) planes. Because of the large interplanar spacing, the lattice planes are easily distinguished thus making clear the onset of disorder should the boundary prove unstable at elevated temperatures. The large planar unit cell allows us to consider this a "generic" boundary as opposed to boundaries with small planar unit cells whose energy is known to be rather sensitive to relative translations of the two halves of the bicrystal.[14] Similarly, we chose a twist rather than a tilt boundary (as is commonly used in the study of the high-temperature stability of grain boundaries[5–9]) because symmetrical tilt boundaries have the smallest planar unit cell possible on a given plane and, hence, are also highly sensitive to translations.[14]

The technical details of the grain-boundary simulations are identical to those described in the previous section except that the runs consisted of 10 000 time steps. In particular, the potential, time step, simulation cell, and number of atoms are the same. The input grain boundary used in the simulations was first relaxed statically at zero temperature and constant (zero) stress in the z direction. Because the perfect stacking of the ideal crystal is destroyed an increase in the interplanar spacing occurs at the grain boundary.

The first grain-boundary simulation discussed here consisted of a total of 10 000 time steps at 900 K with averages compiled over the final 9000 time steps. The average-potential-energy profile is shown in Fig. 6. The effect of region II is the same as in the ideal-crystal simulations. The higher energy of the atoms in the grain boundary is also apparent. The average energy of all atoms more than three planes away from both the grain boundary and region II is -0.8915 eV compared to -0.8937 eV in the 3D ideal crystal; this indicates that the grain boundary is, indeed, embedded in an ideal-crystal environment. Figure 7 shows the average-temperature profile while Fig. 8 illustrates the average interplanar spacings. Averaging the interplanar spacings for the surrounding bulk regions in the same way as the energy, we find an average bulk spacing of $(0.5165+0.0004)a_0$ compared with $(0.5168\pm0.0004)a_0$ in the 3D PBC ideal crystal, again demonstrating the close agreement. In all other properties, the atoms three or four planes removed from the interface behave like ideal-crystal atoms as well.

We note that in the course of the simulation, the grain boundary migrated from an initial position between the 16th and 17th planes to one between the 15th and 16th planes. In the average profiles this migration creates the appearance that the disorder near the grain boundary has spread over a wider spatial region than existed at any given instant. This is seen, for example, in the instantaneous-energy profile which shows only about six

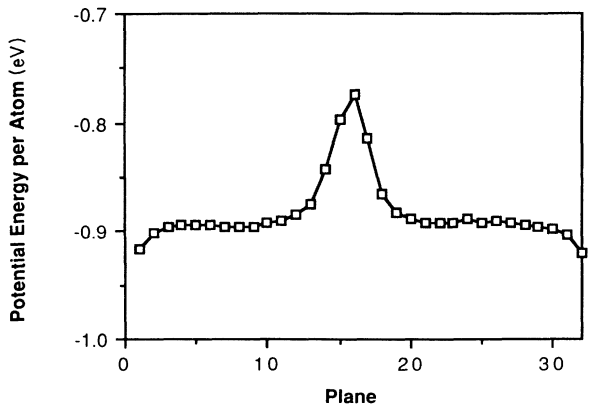

FIG. 6. Average-potential-energy profile for the 2D PBC grain boundary after 10 000 time steps.

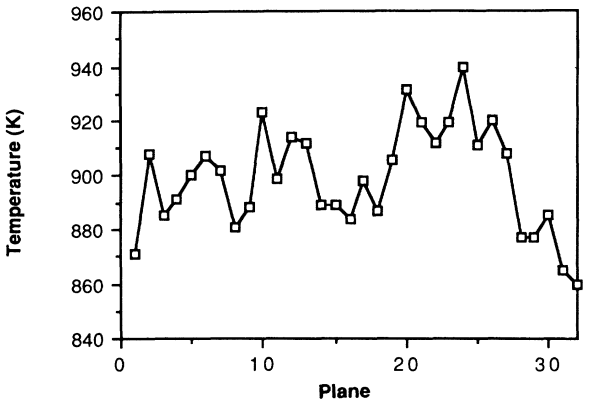

FIG. 7. Average-temperature profile for the 2D PBC grain boundary after 10 000 time steps.

planes affected by the grain boundary as opposed to about eight in the average-energy profile.

Finally, we show the instantaneous structure factor in Fig. 9. Because of the relative rotation of the two halves of the twist-boundary bicrystal, different wave vectors are needed to characterize the planar order in each half. Specifically, if $\mathbf{k}_1$ is the wave vector chosen for the bottom half, then the vector for the top, $\mathbf{k}_2$, is just $\mathbf{k}_1$ rotated by the relative misorientation. Then, at zero temperature, $S(\mathbf{k}_1)$ equals unity in the lower half of the bicrystal and zero in the top half while the reverse is true for $S(\mathbf{k}_2)$. Both quantities are shown in Fig. 9 where it is seen that away from the grain boundary, which is more disordered than the bulk ideal crystal, the system again behaves like an ideal crystal.

We have performed simulations on this system up to 1050 K and at all temperatures find similar behavior as described here. Specifically, the effects of region II are, as in the ideal-crystal simulations, confined to the planes within one to two potential cutoffs of region II. From these results and the results of the previous section, we conclude that the 2D PBC's provide a physically realistic model for the molecular-dynamics simulation of solid interfaces embedded in bulk ideal crystal.

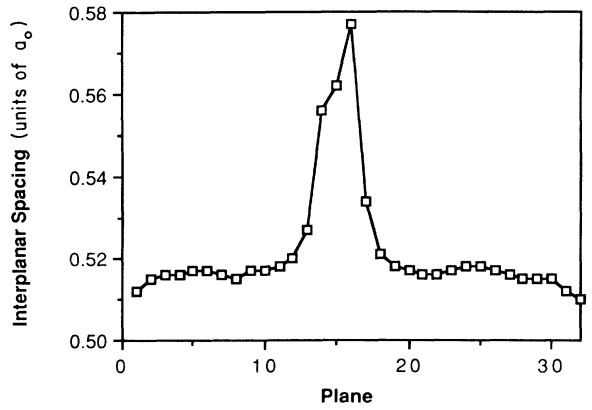

FIG. 8. Average interplanar spacings for the 2D PBC grain boundary after 10 000 time steps.

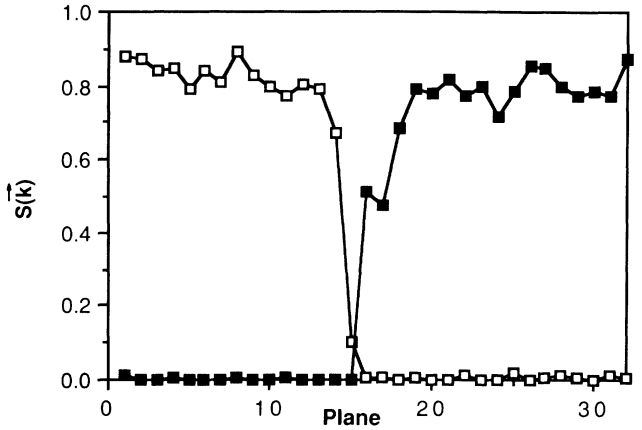

FIG. 9. Instantaneous $S(\mathbf{k})$ profile for the 2D PBC grain boundary, after 10 000 time steps, for the two wave vectors corresponding to the planar symmetry of the lower and upper halves (open and solid symbols, respectively) of the bicrystal.

V. HIGH-TEMPERATURE STABILITY

The 2D PBC model presented in this paper was developed for the study of interfacial systems at high temperature where ordinary 3D PBC's and 2D fixed borders encounter the problems discussed in the introduction. To illustrate its properties and dynamical behavior we have therefore described the equilibration with the 2D PBC model of an ideal crystal and a grain boundary at relatively high temperatures. To enable us to study not only the equilibration but also the kinetics of the grain boundary at these temperatures, the grain-boundary simulations were run twice as long as the ideal-crystal simulations. In particular, the high-temperature stability of the grain boundary was thus investigated.

We noted previously that at the end of the 900 K simulation, the grain boundary has migrated from between the 16th and 17th planes to between the 15th and 16th planes. This is clearly seen in Fig. 10(a) which shows the time variation of the planar structure factors for plane 16. One can see that up to time step 4000 this plane clearly is part of the upper half of the bicrystal. As time progresses further, the symmetry of the plane changes to that of the lower half of the bicrystal, thus signifying migration of the grain boundary. This migration step seems to consist of two stages. First, a plane adjacent to the grain-boundary plane becomes disordered and may remain so for some time. This is followed by recrystallization of the plane into the opposite symmetry state. The nature of the disordered state is unknown at this point. In particular, we do not know if it is liquidlike or solidlike with a structure characterized by different symmetries than that of the bicrystal. During the migration the mean-squared displacement (MSD) of the atoms in the 16th plane, Fig. 10(b), show an almost linear increase with time. However, it is clear that this is necessary whether the disordered state is liquid or solid since substantial atomic rearrangement occurs as the plane changes symmetry. When the migration is complete, the mean-squared displacement is again constant.

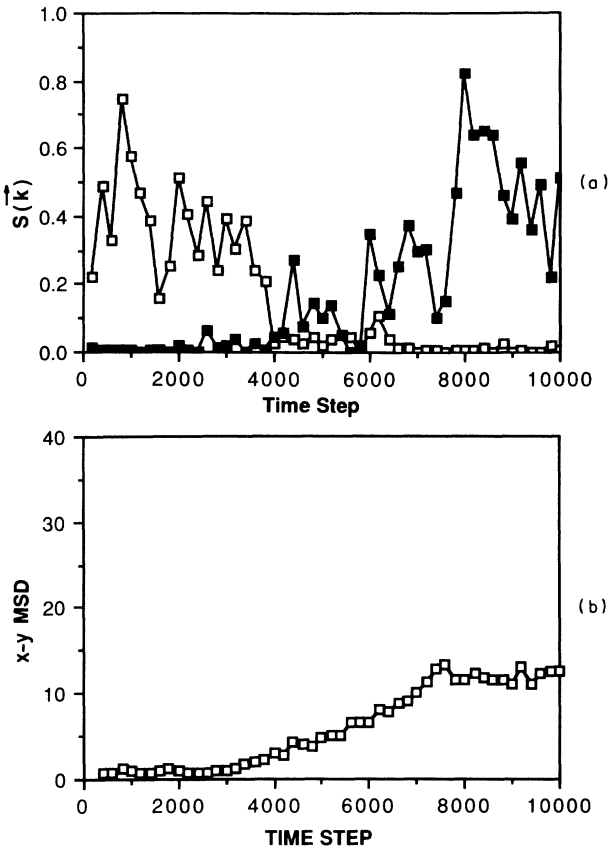

FIG. 10. Part (a) shows the instantaneous $S(\mathbf{k})$ as a function of time for the 16th plane in the 2D PBC grain-boundary system for the two wave vectors corresponding to the planar symmetry of the lower and upper halves (open and solid symbols, respectively) of the bicrystal. Part (b) shows the instantaneous x-y MSD (in unit of $10^{-2}a_0^2$), for the same plane, as a function of time.

To further investigate this problem, we have studied the same system with ordinary 3D PBC's with considerably different results. The system then contains two boundaries and, as for 2D PBC's, in each case, one of the planes adjacent to the boundaries shows a mean-squared displacement which increases roughly linearly with time although the second stage of the migration never takes place. While one boundary never completely disorders, the other disorders considerably with both structure factors fluctuating significantly. The reason for this behavior can be traced to the lack of translational freedom in the system with 3D PBC's. That this is, indeed, the case was confirmed by introducing 2 extra degrees of freedom in the 3D case which allowed for independent translations of the two halves of the bicrystal. (The method for doing this is described in the Appendix.) The interesting result was that migration now took place as in the 2D case. It appears that ordinary 3D PBC's, which, even with a thermostat, do not allow the center of mass of the overall system to move and therefore induce the same translational state in both boundaries, inhibit the migration process. Since it is known that migration and sliding are intimately connected in grain boundaries[15] this coupling between the two boundaries present in 3D PBC simulations thus appears to inhibit the migration process.

Returning to the 2D PBC simulations, we slowly increased the temperature from 900 to 1050 K and extended the simulation at that temperature for another 10 000 time steps. The behavior observed was similar to that at 900 K with the migration occurring more rapidly. Finally, we increased the temperature to 1100 K. At this temperature, the system was stable for approximately 4000 time steps after which it appeared to melt. Throughout the run at 1100 K, Frenkel pairlike defects formed near the boundary in which atoms became mobile, moving into adjacent slices, before eventually returning to their original planes. After 4000 steps, these defects were present in great numbers forming a disordered region around the boundary which spread with time to eventually cover the whole system. It appears that the presence of the structural defect (grain boundary) has lowered the melting point of the system.

Studies[16] have shown that this is probably due to the fact that the grain boundary causes the system to melt at the thermodynamic melting point where the free energy of the liquid is equal to that of the solid. The spontaneous melting of an ideal crystal, however, occurs above this temperature and is dependent on the heating rate, etc.

VI. DISCUSSION

We have presented a new molecular-dynamics model for the simulation of interfacial systems. The model differs from previous models in that 2D periodic borders are employed allowing the simulation of isolated interfaces. Furthermore, the bicrystal is allowed to translate parallel to the interface plane as well as to expand or contract perpendicular to the interface. While in the present model only $H(3,3)$ is allowed to vary, an extension of this model, employing the Parrinello-Rahman method more fully, would also allow the possibility of strain fluctuations which preserve the planar geometry, although we have not attempted this.

Comparisons of the equilibration with 3D PBC's and 2D PBC's have shown that, aside from a more or less expected effect due to the constraint at the region-I–region-II interface, there is no discernable difference in the results. In particular, a detailed comparison of an ideal crystal equilibrated with ordinary 3D PBC's and the 2D PBC model shows virtually no difference in the properties of the equilibrated crystals. Plane-by-plane profiles of the potential energy, interplanar spacing, temperature, and structure factor are also qualitatively similar in the two models indicating little difference in the distribution of these quantities in the systems.

The grain-boundary equilibrations show that the atoms in the region surrounding the grain boundary behave like bulk ideal-crystal atoms in that the average potential energy, interplanar spacing, and structure factors are essentially the same as in the 3D PBC ideal crystal. This is achieved by explicitly distinguishing, in the model, between the spatial inhomogeneity of the interface region

and the homogeneity of the surrounding bulk regions by the introduction of the region-I–region-II scheme. Then, with the interface properly embedded in bulk ideal crystal, we are able to simulate the interface at arbitrarily high temperatures without incurring the problems which beset 3D simulations, such as the annihilation of boundaries, or 2D simulations with fixed borders which permit neither relative translations nor thermal expansion.

The model was illustrated with a study of the high-temperature stability of a grain boundary. Below the melting point, grain-boundary migration was observed to occur via a two-step process in which a plane adjacent to the boundary first entered into a metastable disordered state after which it recrystallized into the opposite crystalline symmetry. This migration appeared to be inhibited with ordinary 3D PBC's. However, when full translational freedom was incorporated into a 3D PBC simulation, the migration again took place. In the case in which the migration step was not completed (ordinary 3D PBC's), the mean-squared displacement of the atoms in a plane adjacent to the boundary increased linearly with time as the atoms passed in and out of the disordered state which is associated with the migration. This leads us to speculate that the "premelting" phenomena previously seen may actually have been the stabilization of the metastable disordered state associated with migration due to the boundary conditions. In the present case, however, as the boundary induces ordinary melting at a temperature around 1100 K, we were able to equilibrate our boundary at 95% of the thermodynamic melting point of the bicrystal and it appears to be stable. Further details of the observed connection between grain-boundary migration and disordering at high temperatures will appear in another publication.

ACKNOWLEDGMENTS

This work was supported by the U.S. Department of Energy, Office of Basic Energy Sciences–Materials Sciences Division, under Contract No. W-31-109-ENG-38. The authors also wish to acknowledge a grant of computer time on the Energy Research Cray XMP at the Magnetic Fusion Computational Center at Lawrence Livermore National Laboratory.

APPENDIX

Here, we wish to show that a new degree of freedom may be added to 3D PBC's to allow the independent translation of the two halves of a bicrystal. The problem is that the motion of the upper and lower halves of the bicrystal is coupled by the periodicity in the z direction. Since we wish to preserve, here, the 3D PBC's, the only way to decouple the x-y motion of the upper and lower halves of the bicrystal is to introduce a new variable. We shall call this variable $\mathbf{T}$, to indicate its similarity to the translation vectors in the region-I–region-II scheme. In the present case, $\mathbf{T}$ is a strictly two-dimensional vector in the x-y plane (parallel to the interface plane). To introduce it, we first write the 3D PBC potential as

$$V_T(\{\mathbf{q}_i\})=\tfrac{1}{2}\sum_{i\neq j}V(\tilde{q}_{ij}) , \qquad =\tfrac{1}{2}\sum_{i\in j}V(\underline{H}\cdot\tilde{\mathbf{s}}_{ij}) , \tag{A1}$$

where $\underline{H}$ and $\{\mathbf{s}_i\}$ were defined in Sec. II. The tilde in (A1) indicates the periodic boundary conditions

$$\tilde{s}_{ijz}=s_{ijz} \quad \text{if } |s_{ijz}|<0.5 , \qquad \tilde{s}_{ijz}=s_{ijz}-1 \quad \text{if } 1.0>s_{ijz}>0.5, \text{ etc.} , \tag{A2}$$

and similar equations hold for the x and y components of $\mathbf{s}_{ij}$. For convenience, Eq. (A2) may be rewritten in terms of a modulus function

$$\tilde{s}_{ijz}=\mathrm{mod}(s_{ijz},0.5) , \tag{A3}$$

so

$$\tilde{s}_{ijx}=\mathrm{mod}(s_{ijx},0.5) , \qquad \tilde{s}_{ijy}=\mathrm{mod}(s_{ijy},0.5) . \tag{A4}$$

We summarize these by writing

$$\tilde{\mathbf{s}}_{ij}=\mathrm{mod}(\mathbf{s}_{ij},0.5) . \tag{A5}$$

To introduce the $\mathbf{T}$ vector, we first define a parameter, λ_{ij}, by

$$\lambda_{ij}=0 \quad \text{if } s_{ijz}=\tilde{s}_{ijz} , \qquad \lambda_{ij}=1 \quad \text{if } s_{ijz}>\tilde{s}_{ijz} , \qquad \lambda_{ij}=-1 \quad \text{if } s_{ijz}<\tilde{s}_{ijz} , \tag{A6}$$

so that λ_{ij} tells us whether or not two particles are interacting across the z border. With this definition, the $\mathbf{T}$ vector is introduced by modifying Eq. (A5) as follows:

$$\tilde{\mathbf{s}}_{ij}\rightarrow\mathrm{mod}(\mathbf{s}_{ij}+\lambda_{ij}\mathbf{t},0.5) \quad \text{with } \mathbf{T}=\underline{H}\cdot\mathbf{t} . \tag{A7}$$

Explicitly,

$$\tilde{s}_{ijx}\rightarrow\mathrm{mod}(s_{ijx}+\lambda_{ij}t_x,0.5) , \qquad \tilde{s}_{ijy}\rightarrow\mathrm{mod}(s_{ijy}+\lambda_{ij}t_y,0.5) , \qquad \tilde{s}_{ijz}\rightarrow\mathrm{mod}(s_{ijz},0.5) , \qquad \lambda_{ij}=0 \quad \text{unless } \tilde{s}_{ijz}\neq s_{ijz} . \tag{A8}$$

Equations (A1) and (A8) define the dynamics of the system. At constant volume, the equation of motion for $\mathbf{T}$ is

$$M_T\ddot{\mathbf{T}}=\tfrac{1}{2}\sum_{i\neq j}\left[\frac{\partial V(\tilde{q}_{ij})}{\partial\tilde{q}_{ij}}\frac{\tilde{\mathbf{q}}_{ij}}{\tilde{q}_{ij}}\right]\lambda_{ij} , \qquad M_T\ddot{T}_z=0 , \tag{A9}$$

which, because of the definition of λ_{ij}, shows that the $\mathbf{T}$ vector moves in response to the x and y components of the net force acting across the z border. Therefore, the two halves of the bicrystal may translate independently parallel to the interface plane and the T vector will move so as to assure that no net x-y force acts across the z border. Except for the change in the periodic border conditions indicated by Eq. (A8), the equations of motion for the particles are unchanged. In addition, this system is conservative and easily incorporated into the Parrinello-Rahman scheme. It does, however, suffer from the 3D PBC problem of introducing two boundaries into the unit cell.

*Permanent address: Department of Nuclear Engineering, Massachussetts Institute of Technology, Cambridge, MA 02139.

[1]F. F. Abraham, Adv. Phys. **35**, 1 (1986).

[2]M. K. Baskes, M. S. Dao, B. Dodson, and S. Foiles, Mater. Res. Soc. Bull. **8**, No. 2, 28 (1988).

[3]See, for example, R. J. Harrison, G. A. Bruggeman, and G. H. Bishop, in *Grain Boundary Structure and Properties,* edited by G. A. Chadwick and D. A. Smith (Academic, London, 1976), Chap. 2; P. D. Bristowe, J. Phys. (Paris) Colloq. **6**, 33 (1982); D. Wolf, Acta Metall. **32**, 245 (1983).

[4]M. Parrinello and A. Rahman, J. Appl. Phys. **52**, 7182 (1981).

[5]G. Ciccotti, M. Guillope, and V. Pontiis, Phys. Rev. B **27**, 5576 (1983); M. Guillope, G. Ciccotti, and V. Pontikis, Surf. Sci. **144**, 67 (1984); M. Guillope, J. Phys. (Paris) **47**, 1347 (1986).

[6]F. Carrion, G. Kalonji, and S. Yip, Scr. Metall. **17**, 915 (1983); P. Deymier, G. Kalonji, R. Nejafabadi, and S. Yip, Surf. Sci. **144**, 77 (1984).

[7]P. S. Ho, T. Kwok, T. Nguyen, C. Nitta, and S. Yip, Scr. Metall. **19**, 993 (1985); T. Nguyen, P. S. Ho, T. Kwok, C. Nitta, and S. Yip, Phys. Rev. Lett. **57**, 1919 (1986).

[8]P. Deymier, Ph.D. thesis, Massachusetts Institute of Technology, 1985; P. Deymier, A. Taiwo, and G. Kalonji, Acta Metall. **35**, 2719 (1987).

[9]J. W. Broughten and G. H. Gilmer, Phys. Rev. Lett. **56**, 2692 (1986).

[10]C. Rottman, J. Phys. (Paris) Colloq. (to be published).

[11]G. Bishop, R. Harrison, T. Kwok, and S. Yip, J. Appl. Phys. **53**, 5596 (1982).

[12]D. Wolf, J. Am. Cer. Soc. **67**, 1 (1984).

[13]D. Wolf, in *Computer Simulation in Material Science,* edited by R. J. Arsenrault, J. R. Beeler, and D. M. Esterling (American Society of Metals, Metals Park, OH, 1987), pp. 111ff.

[14]D. Wolf, J. Phys. (Paris) Colloq. **64**, C4-197 (1985).

[15]M. F. Ashby, Surf. Sci. **31**, 498 (1972).

[16]S. R. Phillpot, J. F. Lutsko, and D. Wolf (unpublished).